air, where changes in the surface tension occur with changes in electric field, appears to be an example of a generalized electrocapillary type system. The second ion accumulation mechanism may be more applicable to the situation in natural membranes where appreciable transference does occur under the influence of an electric field. This mechanism may cause transient changes in the concentration of ions at the inside or outside membrane surface when one imposes electric fields across natural membranes to induce an impulse (for example, action potential in nerves). This has been suggested (7) in an initial attempt to formulate relevant physical mechanisms for excitable membranes.

MARTIN BLANK
STEVEN FEIG
Department of Physiology, Columbia University, College of Physicians and Surgeons, New York 32

References and Notes

1. J. T. G. Overbeek, in *Colloid Science*, H. R. Kruyt, Ed. (Elsevier, Amsterdam, 1952), vol. 1, pp. 146–165.
2. W. Nernst and E. H. Riesenfeld, *Ann. Physik.* **8**, 600 (1902).
3. Supported by a grant GM-10101 and a research career development award GM-K3-8158 from the U.S. Public Health Service. One of us (S.F.) was a part-time research fellow in the physiology department, 1960–1961. We thank Miss B. Bao for technical assistance.
4. J. T. Davies, *J. Phys. Chem.* **54**, 185 (1950).
5. J. Guastalla, in *Proc. Intern. Congr. Surface Activity, 2nd, London*, J. H. Schulman, Ed. (Butterworth, New York, 1957), vol. 3, p. 112.
6. R. M. Hurd, G. M. Schmid, E. S. Snavely, *Science* **135**, 791 (1962); G. M. Schmid, R. M. Hurd, E. S. Snavely, *J. Electrochem. Soc.* **109**, 852 (1962).
7. M. Blank, *Federation Proc.* **22**, 174 (1963).

2 July 1963

Cavity Formation in Thin Films of Viscous Liquids

Abstract. *High-speed photography was utilized to observe the dynamic growth behavior of a cavity in a viscous liquid. From these observations it has been shown that a relatively elementary analytical approach will reproduce the general cavity growth characteristics.*

The analysis of devices utilizing thin viscous films is often complicated by the occurrence of flow separation. Because of the resulting "free boundary" of the liquid-gas interface, it becomes necessary to furnish additional boundary conditions over those required for the more common problem with fixed boundaries. To gain an insight into the circumstances contributing to the formation of these cavities, a combined experimental and analytical program was initiated. This report is a summary of the results of this program, which were presented at the 1962 General Motors Research Laboratories symposium, Cavitation in Real Liquids (*1*).

In the experimental program cavities were formed by pulling apart two parallel surfaces between which was entrained a viscous liquid. From observations of the growth patterns of these cavities, it was possible to compare the analytical results based upon thin-film approximations with the actual cavity growth.

One of the two surfaces used in the cavity growth process was an optical flat 2 inches (about 5 cm) in diameter. Its mounting fixture was constrained by two flexure plates so as to be always parallel to a ground steel surface. The initial separation between the surfaces was of the order of 0.0005 cm. A motor-driven cam forced the surfaces apart at a rate which was sufficient to initiate the growth of a cavity while the area surrounding the optical flat was continuously flooded with a viscous liquid. The initiation, growth, and collapse of the cavities occurred in about 0.5 second, at which time the separation width was approximately 0.089 cm. A continuous record of the plate separation width was obtained through the use of a preloaded cantilever beam transducer element which bore upon a steel pin which passed through the optical flat holder and made contact with the steel surface. A high-speed camera was used to record the cavity formation at 7000 frames per second, the pictures being taken through the optical flat.

Since films of the order of 0.0025 cm are extremely difficult to observe, even with dyes added, it was necessary to use a material which would fluoresce under ultraviolet light. The liquid used was a petroleum base fluid which has a viscosity of 15 centistokes at 26.7°C, a surface tension of 34.9 dyne/cm at 23.3°C, and a specific gravity of 1.008 at 15.6°C.

Because of the symmetry of the system, as the surfaces are separated one might expect to find a lowering of the pressure within the film until a cavity was formed at the center of the disk, when the cavity would expand with polar symmetry until the time it collapsed. This did not prove to be correct. There was no single cavity formation; instead, there were many small circular voids which occurred at random over the surface of the optical

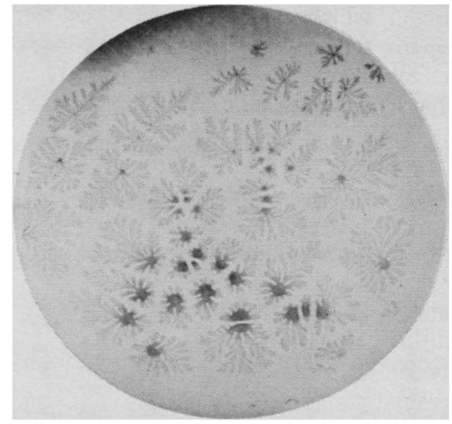

Fig. 1. The growth of cavities in a thin film of a viscous liquid between two parallel plates. The fracturing cavity front assumes a dynamic fern-like structure with increasing time.

flat. This phenomenon can be attributed to the effects of surface defects acting as nucleation sites and of the presence of dissolved gases in the fluid. Various areas within the film are capable of sustaining different levels of reduced pressure before a cavity forms because of local conditions existing in the film. Consequently, as the pressure is lowered, this local threshold value for cavity formation may occur at several locations in the film before the effect of the aggregate cavities precludes the formation of new voids. The continued growth of each circular void was marked by a fracturing of the cavity front and by the extension of radial runners, as shown in Fig. 1. From these radial growth patterns there appeared many subordinate finger-like appendages growing, in general, at an angle inclined to the growth direction of the radial arterial extensions. The interactions of these extremely unstable

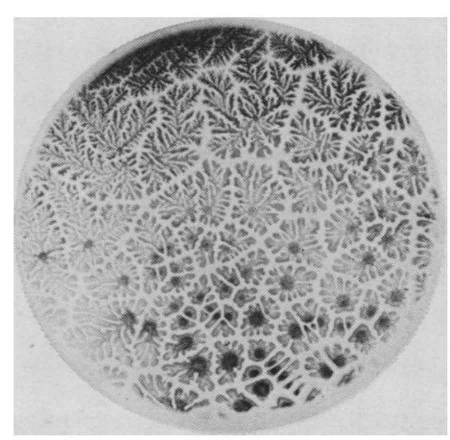

Fig. 2. The coalescence of many separate cavities into one circular cavity. The residual oil appears in the form of filaments throughout the cavity area.

fern-like structures slowed down the rate at which they propagated in the regions separating several cavities and the visual effect was a growth pattern which moved toward the periphery of the disk. There was then a period of coalescence, the many cavities merging into one well-defined circular cavity as shown in Fig. 2. Although many filaments of the liquid remained in this region, their static nature would indicate the existence of a constant pressure within the area. It was not possible to determine whether these filaments of residual fluid were clinging to the optical flat or if they extended between the two surfaces. A further separation of the surfaces caused the cavity to collapse. This was an extremely stable phenomenon, the receding boundary wiping out the residual fluid filaments and circular symmetry being maintained until the collapse phase was complete.

The analytical work was based upon the assumptions of (i) laminar flow, (ii) constant viscosity, (iii) an incompressible fluid, (iv) no slip at the solid-liquid boundary, (v) a film thickness h smaller than other dimensions of the system, (vi) a negligible effect of inertia terms, surface tension, and residual fluid in the cavity, and (vii) the cavity boundary being a single circle concentric with the disk. Although the last assumption is not in accord with the observed initial growth pattern, it is realistic for the later stages of the cavity growth. The restrictions of assumption vi can be removed and first-order approximations to the effects of inertia and surface tension can be included without any mathematical hardships. Because of the relative slowness of this cavity formation, in contrast to cavitation phenomena which may be measured in milliseconds, the effect of fluid inertia does not appreciably alter the calculated results. With thin film approximations, a first-order differential equation was obtained for the time rate of change of the cavity radius B, as a function of the disk radius R, the viscosity μ, the film thickness h, the atmospheric pressure p_a, and the cavity pressure p_v:

$$\dot{B} = \frac{h^2}{12\,\mu\, B\, \ln\,(B/R)} \times \left[P_a - P_v - \frac{3\,\mu\,\dot{h}}{h^3}\,(R^2 - B^2)\right] - \frac{\dot{h}\,B}{2h}$$

By using the recorded data for h and starting the numerical integration of the differential equation at a time when a small cavity was observed experimentally, a theoretical cavity was obtained which is compared with the observed cavity in Fig. 3. The measured curve for the early stages of cavity growth is based upon an equivalent circular area and, as expected, does not follow too closely the calculated curve. However, for the period where the experimental cavity is circular and assumption vii is fulfilled, there is excellent correlation between measured and calculated values.

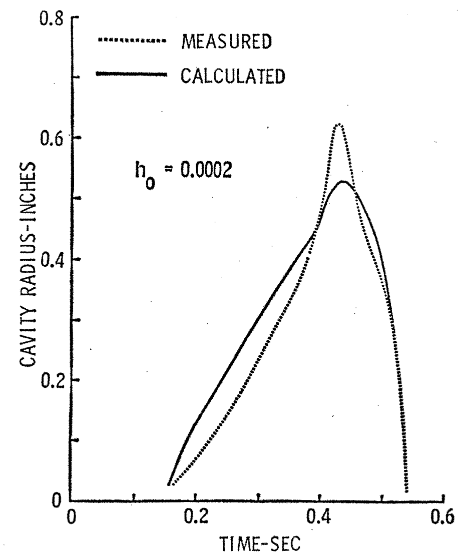

Fig. 3. A comparison between the measured and the calculated cavity radius.

DONALD F. HAYS
JAMES B. FEITEN

General Motors Research Laboratories, Warren, Michigan

Note

1. The proceedings of the symposium are to be published by the Elsevier Publishing Co.

10 June 1963

Magnetite: Preferred Orientation on the Basal Plane of Partially Reduced Hematite

Abstract. *Crystallites of two different orientations have been observed in the polycrystalline magnetite layer formed by carbon monoxide reduction on the basal plane of a hematite single crystal. The relative reducibility of hematite and magnetite ores may be related to this double orientation.*

Blackman and Kaye (*1*), in an electron diffraction study of partially reduced single crystals of hematite (α-Fe_2O_3), found preferred orientation in the surface layer of polycrystalline magnetite (Fe_3O_4) which was formed on the hematite basal plane. Their reductions were carried out by thermal dissociation at 700° and 1000°C. The orientation reported by them is: (111) magnetite parallel to (00·1) hematite, and $[1\bar{1}0]$ magnetite parallel to $[1\bar{1}0]$ hematite (*2*).

This orientation would result from a topochemical reaction which maintains the close-packed oxygen layers in the magnetite crystals parallel to those in the hematite crystal. It also agrees with observations of preferred orientation in hematite formed by the oxidation of magnetite (*3*).

In our work, single crystals of hematite (*4*) were reduced by two different methods. In the first of these, a crystal was heated in air at a pressure of 2×10^{-3} mm-Hg and a temperature of 1200°C for 1 minute. The resulting magnetite layer was 1 to 3 μ thick. In the second method, a crystal was reduced in a mixture of 30-percent CO, and 70-percent CO_2 at 1 atm and 657°C for 1 minute. The magnetite layer was 12 to 15 μ thick.

Back-reflection x-ray diffraction patterns from the basal planes of the crystals were recorded photographically with radiation from a cobalt-target tube. These patterns consisted of a superposition of the Laue pattern of the hematite crystal and a portion of the Debye-Scherrer pattern of the magnetite layer. The indexes of the three observed rings in the Debye-Scherrer pattern were 555, 662, and 840. These rings showed the nonuniform intensity distribution about their circumferences that is typically associated with preferred orientation. From an analysis (*5*) of the intensity distribution within the 840 ring as a function of the angle between the normal to the basal plane and the direction of the incident x-ray beam, a (210) pole figure was plotted for each crystal. The pole figure for the crystal reduced by thermal dissociation is shown in Fig. 1. The six symmetrically related areas of high-pole density arise from the orientation reported by Blackman and Kaye (orientation I). The pole figure for the crystal reduced in the CO atmosphere is shown in Fig. 2. The six areas of high-pole density resulting from orientation I are repeated here and, in addition, subsidiary maxima surround each of these principal high density regions. These subsidiary maxima arise from a second, less prominent orientation (orientation II) in which (211) magnetite is parallel to (00·1) hematite, and $[\bar{1}11]$ magnetite is parallel to [010] or $[0\bar{1}0]$ hematite.